23rd ABCM International Congress of Mechanical Engineering
December 6-11, 2015, Rio de Janeiro, RJ, Brazil

BIFURCATIONAL PHENOMENA IN A NONIDEAL CRANK-SLIDER MECHANISM COUPLED TO THE SUPPORT OF A PHYSICAL PENDULUM

Rafael Henrique Avanço
Hélio Aparecido Navarro
Department of Mechanical Engineering, University of São Paulo, Av. Trabalhador São-carlense, nº400, São Carlos, SP, 13566-590, Brazil.
avanco@sc.usp.br
han@sc.usp.br

Átila Madureira Bueno
UNESP Sorocaba, Control and Automation Engineering
atila@sorocaba.unesp.br

Reyolando Manoel Lopes Rebello da Fonseca Brasil
Federal University of ABC
reyolando.brasil@gmail.com

José Manoel Balthazar
Department of Mechanical Engineering (ITA)
jmbaltha@gmail.com

Abstract. *A pendulum system with a fixing point that is vibrated in the horizontal plane is considered. The DC motor, that generates the horizontal plane vibration, is considered to be a limited power source. When operating in low speed of the motor is nonideal, since the speed of the motor is influenced by the pendulum's dynamics. The qualitative description and understanding of the pendulum's planar oscillations under nonideal excitation is studied. In that situation the system presents a considerable variety of nonlinear oscillations. Additionally, a large number of numerical simulations with different initial conditions and numerical values of the physical parameters of the problem are carried out. In non-ideal conditions this dynamical system presents regions of low and high instability, characterized by nonlinear phenomena: quasiperiodic motion, subharmonic oscillations and bifurcational behaviour in the case of small variations of the control parameters. The analysis of these phenomena is performed considering Poincare Maps, phase portraits and time histories.*

Keywords: *Cranck-slider mechanism, pendulum, limited power supply*

1. INTRODUCTION

Dynamical systems are present in several areas, which may include: mathematics, mechanics, electromagnetism, and biology, where, for example, we might mention population growth. Recently, the nonlinear dynamics has been object of increasingly number of research analysis. These papers bring the dynamical behavior of nonlinear dynamical systems through: phase portraits, Poincaré sections, time histories, bifurcation diagrams, Lyapunov exponents and basins of attractions.

The appearance of chaos has been considered of special attention. One of the first to observe the chaos in dynamical system was Edward Lorenz with the attempt to forecast the weather. The Lorenz strange attractor is, still today, the classical example of the chaotic dynamics. The occurrence of chaos can be due to phenomena related to the loss of stability in a bifurcation point. These phenomena are: intermittency, period doubling cascade and quasiperiodicity. The study of those phenomena is justified by the search for control methods near the resonance regions. The right choice of control parameters could solve the problem of instability leading the dynamical system to a desired motion.

In mechanical systems, the classical parametric pendulum is extensively analyzed in literature about its chaotic dynamics. Leven and Koch (1981) were the first the check the chaos in the pendulum harmonically excited in the vertical direction. They discovered that under specific values of frequency and amplitude of excitation provoke the chaotic movement of the mechanism.

In Kransnopolskaya and Shvets (1990), Belato et al (2001) and Krasnopolskaya and Shvets (1993), it was analyzed the mechanism represented in Fig(1), where a crank-slider mechanism powered by a DC motor moves horizontally the point of suspension of a pendulum. The idea in those analysis performed was to consider the effect of “feedback” present in mechanisms with limited power supply. In Krasnopolskaya and Shvets (1990), the steady state of the pendulum dynamics is analyzed where The voltage of the DC motor is parameter of control. Near the resonance region, the pendulum exhibited different kinds of motion: multi-periodic, quasiperiodic and chaotic. In Krasnopolskaya and Shvets (1993), they verified that some regions of chaotic motion occurs only under the consideration of the limited power supply, not being observed when the ideal excitation is present. Also in Krasnopolskaya and Shvets (1993), it was found the chaos in piezoelectric vibrators excited by a generator with limited power.

The same mechanism, when analyzed in Belato et al (2002), where using the Hamilton's equations it was possible to reach the result of principal solutions of the system through polynomial functions describing the dynamics of the pendulum in stable regions.

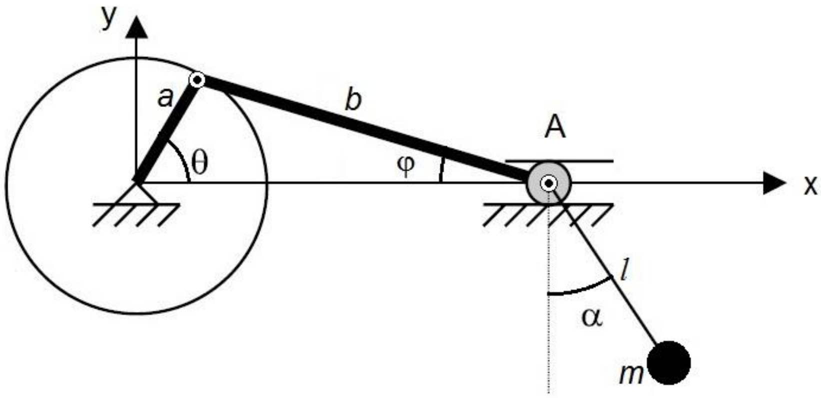

Figure 1. Crank-slider mechanism linked to a pendulum

2. DYNAMICAL MODEL

The dynamical system consists of a DC motor and a disc with moment of inertia J exciting horizontally the point of suspension of the pendulum. The mechanism is a crank-shaft-slider moving a pendulum, where the pendulum has a mass m and the length l. The radius of the crack is represented by the letter$a$, and the length of the shaft possess the length b. The angle in the crank is given by θ and in the shaft by φ.

For the obtainment of differential equations of the system through Lagrange theorem, we write the position of the mass m:

$$x = a\cos\theta + b\cos\varphi + l\sin\alpha \tag{1}$$

$$y = -l\cos\alpha \tag{2}$$

Considering that the angle φ has a trigonometric relation with θ, in Eq.(1) it is substituted by what is represented in Eq.(3):

$$\cos\varphi = \left(1 - \frac{a^2}{b^2}\sin^2\theta\right)^{1/2} \tag{3}$$

Hence, the velocities of mass m may be written in term of $\theta$and α, where the dots are derivative with respect to the physical time t :

$$\dot{x} = -a\,\dot{\theta}\,F + l\,\dot{\alpha}\cos\alpha \tag{4}$$

$$\dot{y} = l\,\dot{\alpha}\sin\alpha \tag{5}$$

Where F is a function defined in terms of a, b and θ , as a consequence of the intrinsic trigonometric relation of θ and φ of this mechanism :

$$F = \sin\theta + \frac{a\sin\theta\cos\theta}{b\left(1 - \frac{a^2}{b^2}\sin^2\theta\right)^{1/2}} \tag{6}$$

The kinect energy of the system, including the disc and moment of inertia of the rotor of the motor, and the pendulum is given by Eq. (7):

$$T = \frac{1}{2} J \dot{\theta}^2 + \frac{1}{2} m \left(\dot{x}^2 + \dot{y}^2 \right) \tag{7}$$

Substituting the derivatives of Cartesian coordinates in terms of α and θ:

$$T = \frac{1}{2}\, J\, \dot{\theta}^2 + \frac{1}{2} m \left[\left(-a\, \dot{\theta}\, F + l\, \dot{\alpha} \cos\alpha \right)^2 + \left(l\, \dot{\alpha} \sin\alpha \right)^2 \right] \tag{8}$$

And the potential energy of the pendulum:

$$V_p = -m\, g\, l \cos\alpha \tag{9}$$

Two degrees of freedom are present when it is considered a limited power supply. So the Lagrangian equations are derived in terms of θ and α, where the right hand side of equations represents the nonconservative forces of the system:

$$\frac{d}{dt}\frac{\partial L}{\partial \dot{\alpha}} - \frac{\partial L}{\partial \alpha} = Q_\alpha^{NC} \tag{10}$$

$$\frac{d}{dt}\frac{\partial L}{\partial \dot{\theta}} - \frac{\partial L}{\partial \theta} = Q_\theta^{NC} \tag{11}$$

The diferential equation obtained with the coordinate α and θ are represented by Eq.(12) and Eq.(13):

$$m\, l^2 \ddot{\alpha} - m\, a\, l\, \dot{F}\, \dot{\theta} \cos\alpha - m\, a\, l\, F\, \ddot{\theta} \cos\alpha + m\, g\, l \sin\alpha = Q_\alpha^{NC} \tag{12}$$

$$J\ddot{\theta} + ma^2 F\, \frac{\partial F}{\partial \theta} \dot{\theta}^2 + ma^2 F^2 \ddot{\theta} - maFl\, \ddot{\alpha} \cos\alpha + maFl\, \dot{\alpha}^2 \sin\alpha = Q_\theta^{NC} \tag{13}$$

The right hand side of equations are the nonconservative forces caused by dissipation of energy by friction or duo to the power supplied by DC motor. The parameter c_A is the friction in the slider, c_α is the friction on the joint opposing the swing of the pendulum and M_{motor} is the momentum of the motor:

$$Q_\theta^{NC} = -c_A a^2 F^2 \dot{\theta} + M_{motor} \tag{14}$$

$$Q_\alpha^{NC} = -c_\alpha l^2 \dot{\alpha} \tag{15}$$

In order to find the momentum of the motor, we come back to the idea of the power of a DC motor. The motion of the motor of a continuum current follow the Eq. (16) and Eq. (17):

$$L\, \dot{I} = V - RI - K_E \dot{\theta} \tag{16}$$

$$M_{Motor} = K_T\, I - c_m \dot{\theta} - T_f \tag{17}$$

In the equations above L is the armature inductance, V is the voltage of the motor, K_T is the torque constant and K_E is the voltage constant, c_m is the constant for the internal loss coefficient in the motor and T_f is the constant friction toque in the motor.

The inductance of the armature is neglected duo to the fact that the electrical time constant of the motor L/R is much smaller than the mechanical time constant $J/K_E K_T$. Therefore, the Eq.(16) and Eq.(17) becomes:

$$V = RI + K_E \dot{\theta} \tag{18}$$

$$M_{Motor} = K_T I - c_m \dot{\theta} \tag{19}$$

Substituting the Eq.(14), Eq.(15), Eq.(18) and Eq.(19) in Eq. (12) and Eq.(13), the differential equations of motion are found. However, the time must be dimensionless. So the parameter τ is inserted based on the natural frequency of the pendulum. The apostrophe means the derivative with respect to the dimensionless time τ as represented in the sequence:

$$\tau = \omega_0 t \tag{20}$$

$$\alpha' = \frac{d\alpha}{d\tau} = \frac{1}{\omega_0}\frac{d\alpha}{dt} \tag{21}$$

$$\alpha'' = \frac{d^2\alpha}{d\tau^2} = \frac{1}{\omega_0^2}\frac{d^2\alpha}{dt^2} \tag{22}$$

The equations with the time dimensionless are present in Eq.(23) and Eq.(24):

$$\begin{aligned}(J\omega_0^2 + ma^2F^2\omega_0^2)\theta'' &= -ma^2F\frac{\partial F}{\partial \theta}\omega_0^2\theta'^2 + maFl\cos\alpha\,\omega_0^2\,\alpha'' - maFl\sin\alpha\ \omega_0^2\,\alpha'^2 - c_A a^2F^2\omega_0\theta' \\ &+ M_{Motor} - c_m\theta'\omega_0\end{aligned} \tag{23}$$

$$\alpha'' = \frac{a}{l}\frac{\partial F}{\partial \theta}(\cos\alpha)\,\theta'^2 + \frac{a}{l}F\cos\alpha\ \theta'' - \sin\alpha - \frac{c_\alpha \alpha'}{m\,\omega_0} \tag{24}$$

A complete equation with only dimesionless paramaters is not suitable for now because we have the parameter F and F' varying in the time. So in the present paper some dimensionless parameters will not be inserted in order to not involve simplifications.

Afterwards an analysis considering ideal excitation will be performed still in this paper. For this type of excitation, you would have only to replace, in Eq. (24), the value of θ' by ω. The parameter ω means the angular frequency of the crank Ω divided by the natural frequency of the pendulum ω_0:

$$\omega = \Omega/\omega_0 \tag{25}$$

The dimensionless parameters utilized in this paper are , γ and ω. The parameter ϵ stands for that relation of a/b, γ is a friction coefficient $c_\alpha/(m\,\omega_0)$. The value used for γ, in this paper, is 0.01 and the value used of ϵ are 0.05, 0.233 and 0.45. The value of ω is varied in bifurcation diagrams and it is pointed when necessary. The coefficients of friction c_m and c_A are always neglected.

The other parameters were fixed in: a=0.07 m, l=0.3 m, g=9.81 m/s², $K_T = 0.345$ Nm/A, $K_E = 0.345$ Vs, R=0.85Ω, m=0.2 kg, J=0.001655 kg m².

The initial conditions for the pendulum are zero for speed and position. The time step used for τ was $2.75\ 10^{-3}$.

3. NUMERICAL RESULTS

The bifurcation diagrams are constructed through the variation of the parameter V, which is the voltage of the DC motor. For the diagrams, it was considered the last 5 Poincaré sections for each value of V. The figures also represent the average speedy of crank. The value of regime of the crank speedy was worked out using the mean value of the last 50% during the time integration. For all bifurcation diagrams the time used was τ equals 300. In the sequence bifurcation diagrams were plotted considering the results from a pendulum excited by a crank with constant angular velocity. The time histories, phase portraits and Poincaré sections are calculated for both cases.

3.1 Results for nonideal excitation

In Figure (2), Fig(3) and Fig(4), there are the results obtained from the mechanism excited by limited power supply through the DC motor. Comparing the three bifurcation diagrams, it is possible to see in the resonance near θ' equals 0.5 that the amplitude is greater when the parameter ϵ is greater.

Following the bifurcation diagrams, phase portraits and Poincaré sections of the pendulum were plotted. In most of cases, it was verified that the quasiperiodicity leads to chaos. Varying the voltage the sequence observed is: periodic motion, quasiperiodicity and chaos. In Figure 5(a), the voltage of the motor is in 1.72 Volt and the pendulum exhibits a periodic motion. While in Fig.4(b) the quasiperiodic motion takes place. In Figure 6(a), it is possible to see, because of the density of orbits, that the phase portrait represents a chaotic movement. Finally, for the Fig. 6(b), the graphics shows again a quasiperiodic motion.

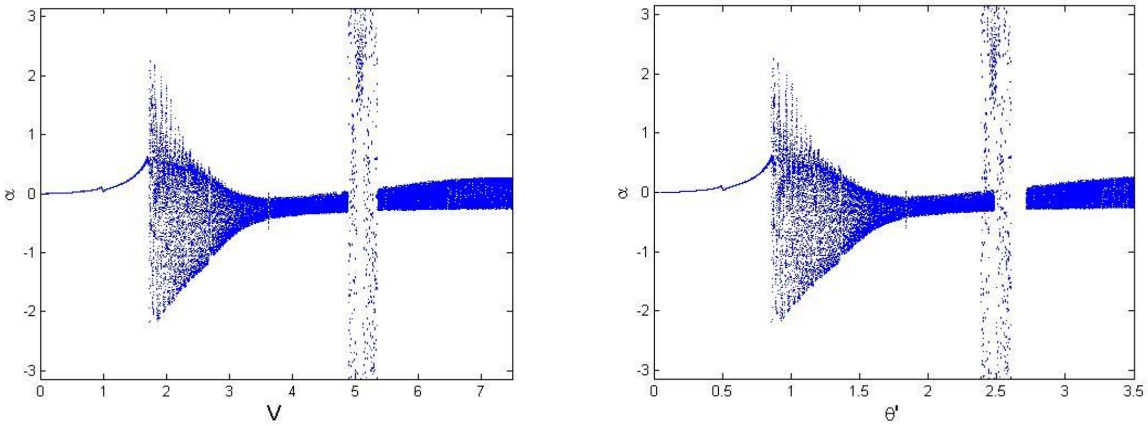

Figure 2. Bifurcation diagram for $\epsilon = 0{,}05$ considering: (a) Voltage (V) (b) Average speed of crank $(\theta^{'})$

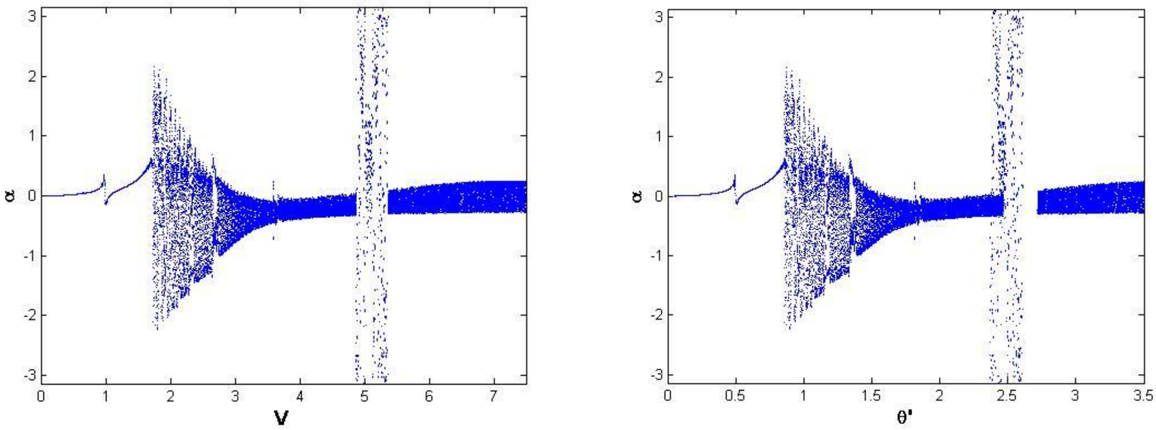

Figure 3. Bifurcation diagram for $\epsilon = 0{,}233$ considering: (a) Voltage (V) (b) Average speed of crank $(\theta^{'})$

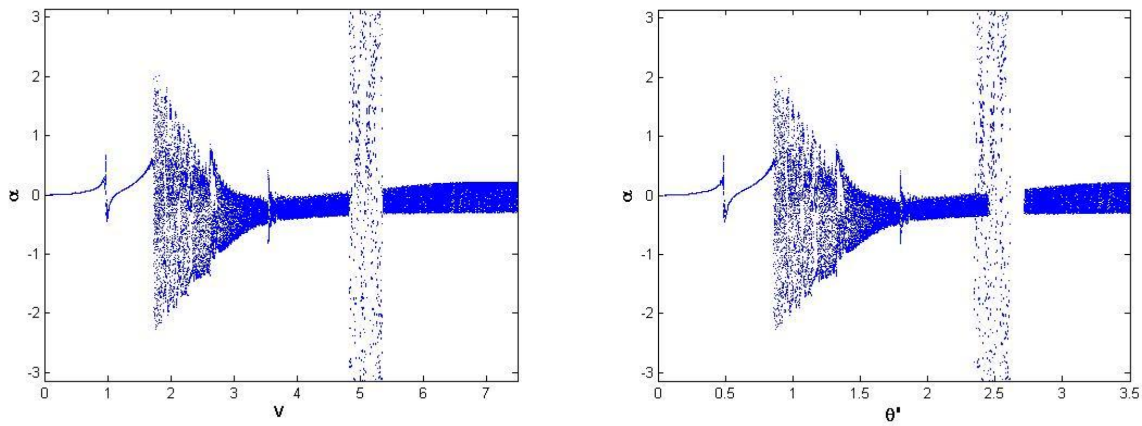

Figure 4. Bifurcation diagram for $\epsilon = 0{,}45$ considering: (a) Voltage (V) (b) Average speed of crank $(\theta^{'})$

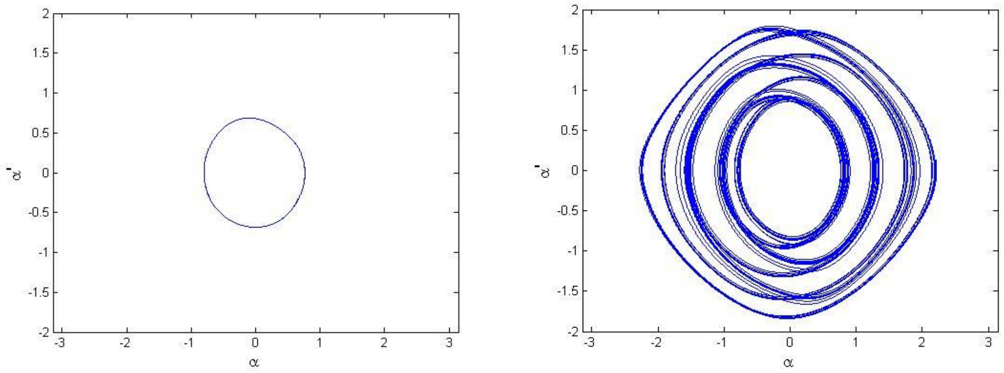

(a) (b)

Figure 5. Phase portraits of the pendulum for different voltage in the motor (a) V=1.72 (b) V=1.736

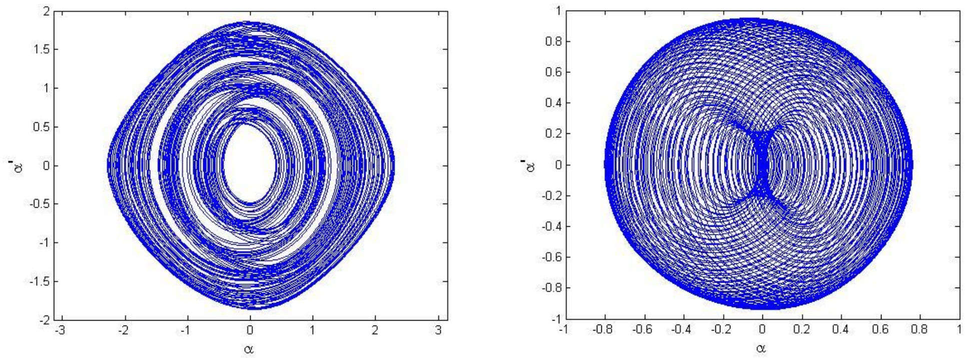

(a) (b)

Figure 6. Phase portraits of the pendulum for different voltage in the motor (a) V=1.75 (b) V=3.0

In the bifurcation diagrams of Fig. 2, Fig. 3 and Fig. 4 demonstrate what could be a instable region near V equals 5 and θ' equals 2.5. Considering this the phase portrait, time history and Poincaré section where constructed. The conclusion was that it was more likely to be a quasiperiodic motion in rotation.

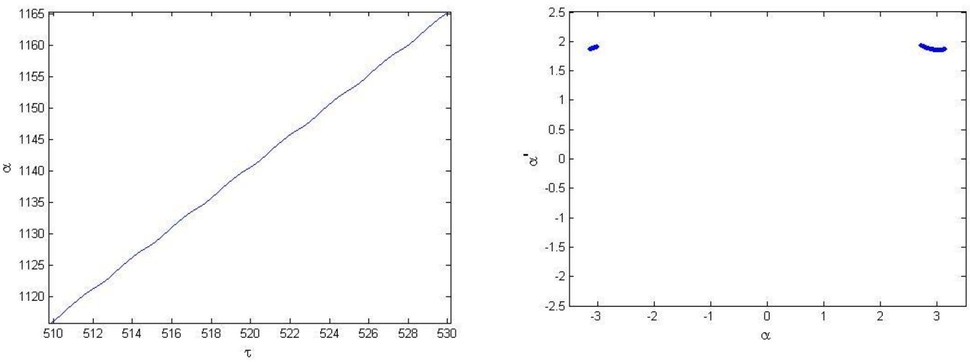

(a) (b)

Figure 7. Pendulum for V equals 5.0 and ϵ equal 0.223 (a) Time history (b) Poincaré section

3.1.1 Basins of attraction for nonideal excitation

Basins of attraction are plotted for different values of the voltage of the DC motor. The area in white represent region where the pendulum does not perform rotations. The blue means that the pendulum started a rotational motion, chaotic or not, maybe mixing oscillations and rotations. For Figure 8(a), the different regions look well determined in their borders. In Figure 8(c), the basin of attraction demonstrates a clear fractal appearance for the blue region. In Figure 8(b) it could be the middle term.

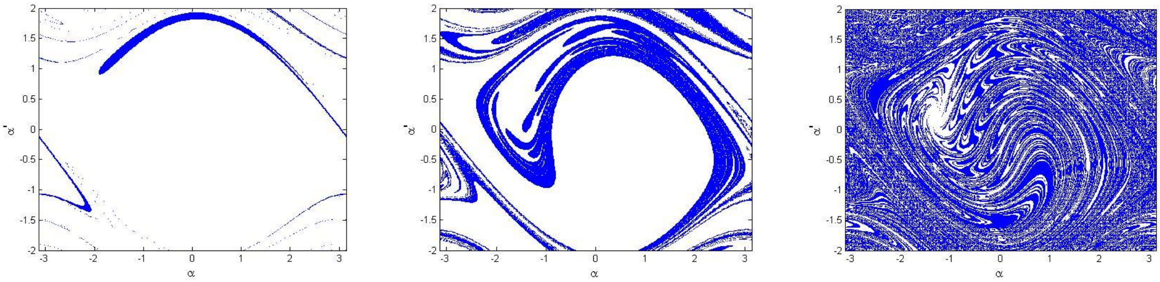

Figure 8. Basins of attraction for different voltage (a) V=1.35 (b) V=1.65 (c) V=1.85

3.2 Results for the ideal excitation

In Figure 9, the bifurcation diagrams, in which the crank performs rotations with constant velocity, are plotted. The interval chosen for ω was equal the values obtained when the voltage of the motor V is varied from 0.1 to 7.5 Volts.

Among the three bifurcation diagrams in Fig. 9, the one where the parameter ϵ is equal to 0.45 has one more resonance zone appearing near the ω equals 1.4. And in the Fig.9(a), where the ϵ is equal to 0.05, the diagram does not show the resonance in ω equals 1.74, where the other two exhibit.

As observed in the nonideal case, the diagrams where the value of ϵ is greater demonstrated greater amplitudes in the resonance zones.

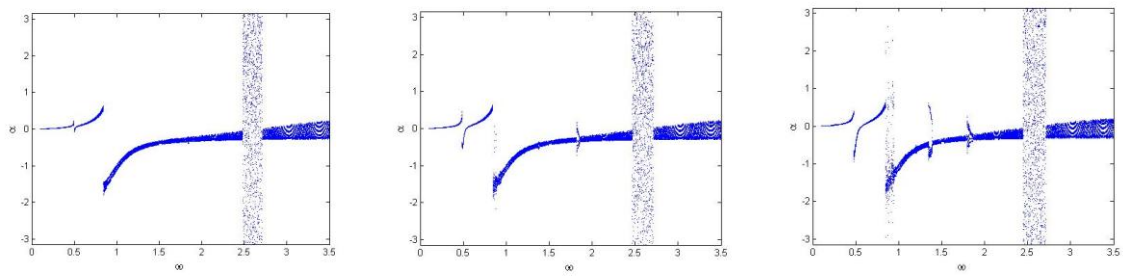

Figure 9. Bifurcation diagrams with ideal excitation for (a) $\epsilon = 0.05$ (b) $\epsilon = 0.233$ (c) $\epsilon = 0.45$

Using time histories, it is verified that different kinds of motion happens with the pendulum in the bifurcation occurred near the ω equal to 2.5. In the Figure 10 (a), the time history of the pendulum, for ϵ equals 0.05 and ω equals 2.5, shows a chaotic behavior. While the Fig. 10(b) demonstrates a rotating solution of the pendulum after a transient chaos. In Figure 11 (a), the pendulum reaches a rotational steady state solution after the transient chaos, whilst the final result in Fig. 11(b) is the oscillatory movement after τ equal to 4050. In Figure 12(a), for ω equal to 2.5, the motion of the pendulum goes to rotating in τ equals 300, and in Fig 12(b), for ω equals 2.6, the chaotic result was maintained for all time simulated.

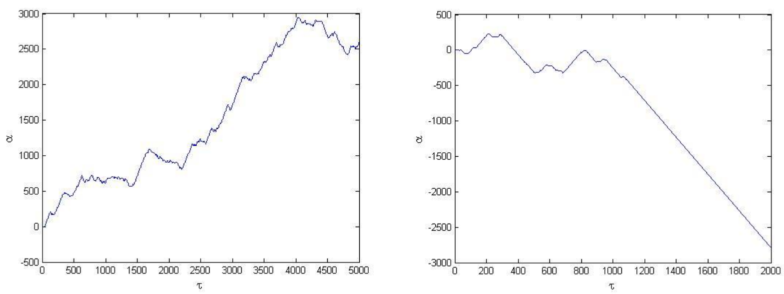

(a) (b)

Figure 10. Time histories of the pendulum for $\epsilon = 0.05$ (a) $\omega = 2.5$ (b) $\omega = 2.6$

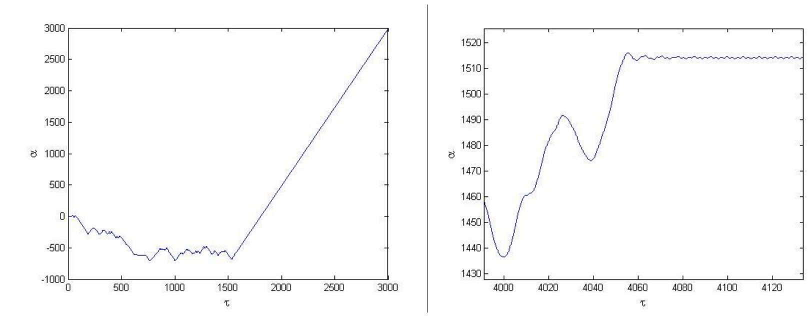

(a) (b)

Figure 11. Time histories of the pendulum for $\epsilon = 0.233$ (a) $\omega = 2.5$ (b) $\omega = 2.6$

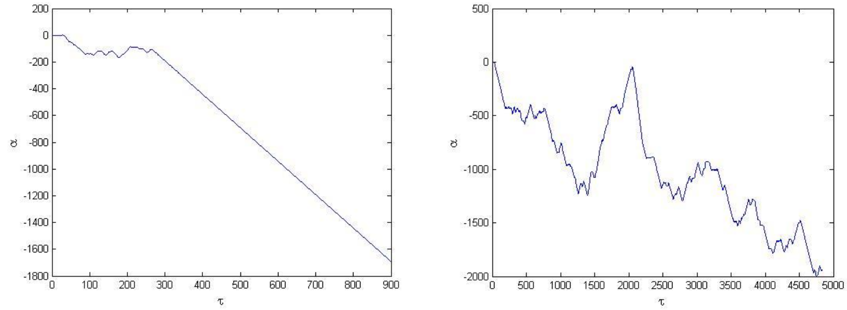

Figure 12. Time histories of the pendulum for $\epsilon = 0.45$ (a) $\omega = 2.5$ (b) $\omega = 2.6$

4. CONCLUSIONS

The main difference between the results of ideal excitation and nonideal when comparing the bifurcation diagrams is presence of the chaos in the oscillatory motion of the pendulum when excited by the DC motor near the frequency θ' equals 1.0. This is not observed in the ideal excitation. The most surprising in the ideal excitation is the mixture of different types of motion near the angular frequency ω equals 2.5.

The future works could base on investigate the same mechanism under limited source of energy, considering a simplified model that demonstrate a reasonable approach still.

5. ACKNOWLEDGEMENTS

The authos are thankful to the Brazilian agencies CNPq, Fapesp and CAPES.

6. REFERENCES

BELATO, D.; WEBER, H.I.; BALTHAZAR, J.M.; MOOK, D.T. (2001) Chaotic Vibrations of a nonideal eletro-mechanical system, **International Journal of Solids and Structures** , Vol.38, pp. 1699-1706.

BELATO, D. (2002) **Análise Não-linear de Sistemas Dinâmicos Holônomos Não Ideais**, Tese de Doutorado, Universidade de Campinas.

KRASNOPOLSKAYA, T.S.; SHVETS, A.Y. (1990) Chaotic interactions in a pendulum energy source system. **Prikladnaya mekhanika**, 26:90-96.

KRASNOPOLSKAYA, T.S.; SHVETS, A.Y. (1993) Chaos in vibrating systems with a limited power-supply, **Chaos**, Vol.3, n.3, American Institute of Physics.

7. RESPONSIBILITY NOTICE

The five authors are the only responsible for the printed material included in this paper.